Feedback-Linearizing Control for Velocity and Attitude Tracking of an ROV with Thruster Dynamics Containing Input Dead Zones

Jordan Boehm[1], Eric Berkenpas[2], Charles Shepard[3], and Derek A. Paley[4]

***Abstract*— This paper presents a dynamics and control framework to accomplish six degree-of-freedom tracking of attitude, velocity, and rotational rate setpoints for a remotely operated vehicle with nonlinear thruster dynamics. The thruster dynamics contain input dead zones that complicate linear state feedback control design, and are compensated with nonlinear control strategies, specifically feedback linearization. Modeling the thruster dynamics in the control design mitigates the input dead zones. Simulations with experimentally obtained thrust parameters show improved reference setpoint tracking when compensating for the thruster dynamics.**

I. INTRODUCTION

Remotely operated vehicles (ROVs) are widespread and versatile, being applicable to deep-sea exploration and mining [1], marine research [2], hull inspection [3], and wreckage surveying [4]. To accomplish these tasks, ROV control is typically accomplished through a variety of methods ranging from direct human-in-the-loop control to autonomous, logic-driven control [5]. Controllers for autonomous or semi-autonomous operation have been designed through a variety of feedback frameworks, including feedback linearization [6], [7], robust control [8], [9], and adaptive control [9], [10].

Most ROV operations are accomplished by semi-autonomous or full human control, whereby direct commands from an operator are either processed by a controller or fed directly to individual thrusters [5]. Direct-controlled ROVs typically have orthogonal thruster configurations that allow for intuitive translations from commands to thrusts, but such actuator placement can complicate the vehicle design. As a result, fewer thrusters are often used, thus limiting maneuverability of the ROV [5]. To maintain generality, we analyze an ROV that has a specific thruster placement configuration to accomplish fully actuated control. An auto-stabilizing control system is assumed to process user commands into setpoints.

J. Boehm is supported by a graduate research fellowship from the National Geographic Society.

[1]Jordan Boehm is a graduate student in the Department of Aerospace Engineering at the University of Maryland, College Park, MD, 20742, USA. jboehm77@umd.edu

[2]Eric Berkenpas is the director of the Exploration Technology Laboratory at the National Geographic Society, Washington, DC, 20036, USA. eberkenp@ngs.org

[3]Charles Shepard is the lead mechanical system designer of the Exploration Technology Laboratory at the National Geographic Society, Washington, DC, 20036, USA. mshepard@ngs.org

[4]Derek A. Paley is the Willis H. Young Jr. Professor of Aerospace Engineering Education in the Department of Aerospace Engineering and the Institute for Systems Research, University of Maryland, College Park, MD, 20742, USA. dpaley@umd.edu

This work is presented with relevance to the application of ROVs to aquatic imaging, the primary function of an ROV under development by the National Geographic Society (NGS) shown in Fig. 1. Underwater filmmaking requires smooth setpoint tracking with human-in-the-loop operations. Reference setpoint attitudes and velocities are typically generated through user input and, for complicated thruster configurations, controllers are capable of effectively tracking commanded trajectories. Often ROVs maintain only active closed-loop control of three or four degrees of freedom, while allowing roll and pitch parameters to be passively stabilized by relying on the natural stability of the vehicle due to the relative locations of the centers of gravity and buoyancy [5], [7], [8], [11]. However, for the purposes of deep-sea imaging, it is useful to have full user control of all attitude parameters, similar to a multi-rotor aerial drone, in order to obtain the desired cinematic effects.

To enhance controller performance and reduce limit-cycle behavior, actuator dynamics are accounted for in the control design [8], [12]. A variety of methods for modeling thrusters for underwater vehicles have been developed in previous work. A two-state axial flow dynamic model [13]–[15] accounts for thrust overshoot but is limited to uni-directional flow characterization. A two-state rotational flow model [16] has no more model accuracy than the axial flow model. Lastly, a multi-directional axial flow model [17] requires a large number of parameters to be identified with extensive system testing. This paper expands upon a single-state voltage-driven thruster model presented in [8]. We consider an analog voltage signal (throttle) as the control input for the thruster dynamics, which also exhibit a dead zone nonlinearity. A single-state dynamic thruster model is valid for low-speed movement [8], [14], [15].

In previous work, robust and adaptive control techniques have been used for dead zone compensation in the absence of well-identified model parameters [18], [19]. This paper utilizes feedback linearization to compensate for nonlinearities in thruster dynamics, because high-quality propeller speed, thrust, and torque data obtained from a six-axis Gough-Stewart platform load cell (Fig. 2) are available [20]. Other techniques [18], [19] for improving the robustness of feedback-linearizing methods are out of the scope of this paper.

The contributions of this paper are (1) a nonlinear control law for throttle-controlled thruster dynamics with input dead zones using experimentally obtained parameters; and (2) implementation of a feedback-linearizing and dead-zone-compensating thruster controller for the six degree-of-

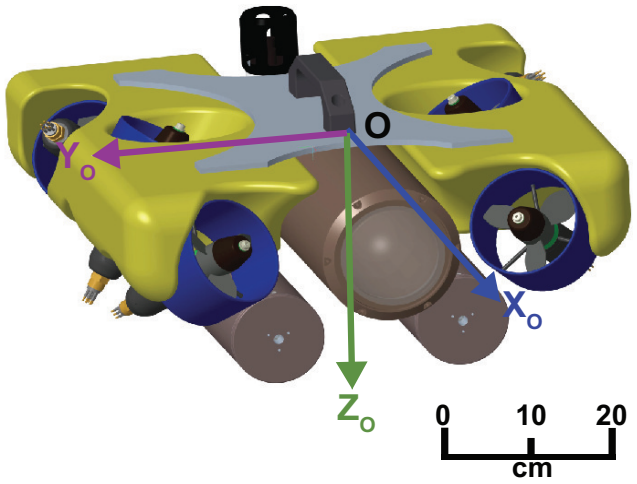

Fig. 1. Computer rendering of the ROV under development by the National Geographic Society. Body-fixed reference frame axes are marked.

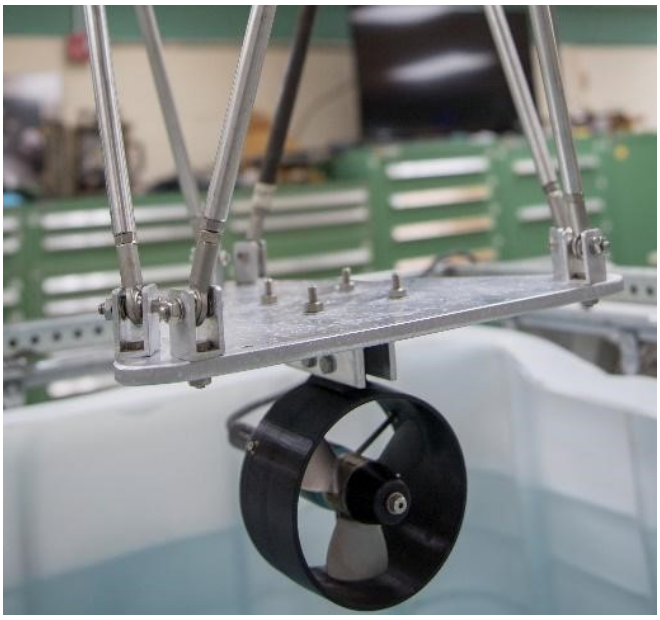

Fig. 2. Six-axis Gough-Stewart platform testbed setup instrumented with six load cells used for system identification of an ROV thruster [20].

freedom (DOF) attitude and speed setpoint tracking of an ROV with throttle-controlled thruster dynamics. In addition, we illustrate the closed-loop control results through simulation and compare these to an alternative thruster controller based on a lookup table that does not account for actuator dynamics. Ongoing work seeks to experimentally demonstrate the results on an ROV testbed currently under development (see Fig. 1).

The organization of this paper is as follows. Section II presents the full six DOF equations of motion for a rigid-body ROV and a feedback-linearizing thrust control law to stabilize the setpoint-tracking dynamics of the system. Section III presents the rotor-speed dynamics of the thrusters and proposes a nonlinear analog throttle signal control law to achieve stability of setpoint tracking. Section IV combines the control methods of the previous sections into the full state model. Closed-loop performance is illustrated through simulation and comparison to a controller with uncompensated thruster dynamics. Section V summarizes the paper and discusses ongoing work.

II. ROV DYNAMICS AND CONTROL

The rigid-body dynamics of an underwater vehicle including hydrodynamic drag and added mass parameters defined in a body-fixed reference frame are [21]

$$M\dot{\boldsymbol{\nu}} + C(\boldsymbol{\nu})\boldsymbol{\nu} + D(\boldsymbol{\nu})\boldsymbol{\nu} + \boldsymbol{g}(\boldsymbol{\eta}) = \boldsymbol{\tau} \tag{1}$$

$$\dot{\boldsymbol{\eta}} = J(\boldsymbol{\eta})\boldsymbol{\nu}, \tag{2}$$

where the portion of the state vector describing body frame linear velocities (u, v, and w) and angular velocities (p, q, and r) is given by $\boldsymbol{\nu} = [u, v, w, p, q, r]^T$, and the terms describing position and orientation of the body frame with respect to the Earth-fixed frame are $\boldsymbol{\eta} = [x, y, z, \phi, \theta, \psi]^T$, where x, y, and z are Earth-fixed position coordinates and ϕ, θ, and ψ are the 3-2-1 Euler angles of roll, pitch, and yaw, respectively [11]. If absolute position or orientation are not relevant, some or all of the Earth-relative states may be omitted from the full state vector. We consider the task of setpoint control, where the Earth-relative coordinates x, y, and z are not included in the state feedback control. Therefore, we use the attitude-only state vector, $\boldsymbol{\eta} = [\phi, \theta, \psi]^T$.

M denotes the diagonal mass and inertia matrix including added mass and inertia parameters, $C(\boldsymbol{\nu})$ is the nonlinear Coriolis and centripetal matrix, $D(\boldsymbol{\nu})$ is the diagonal linear and quadratic hydrodynamic drag matrix, $J(\boldsymbol{\eta})$ is the transformation matrix describing attitude rate of the vehicle body-fixed frame relative to the Earth-fixed frame, and $\boldsymbol{g}(\boldsymbol{\nu})$ is the restoring force and moment vector that combines gravitational and buoyancy effects. Additionally, the external force/moment vector is treated as the control input, defined as [21]

$$\boldsymbol{\tau} = K_t \boldsymbol{T}, \tag{3}$$

where K_t is the thruster configuration matrix that describes the orientation of each thruster and $\boldsymbol{T}$ is the vector of input thrusts.

Martin and Whitcomb [6] define the following feedback-linearizing control law, assuming perfect knowledge of vehicle states:

$$\begin{aligned}\boldsymbol{T} = K_t^{-1}[&C(\boldsymbol{\nu})\boldsymbol{\nu} + D(\boldsymbol{\nu})\boldsymbol{\nu} + \boldsymbol{g}(\boldsymbol{\eta}) + M(\dot{\boldsymbol{\nu}}_d \\ &- K_P(\boldsymbol{\eta})\boldsymbol{\Delta\eta} - K_D\boldsymbol{\Delta\nu})],\end{aligned} \tag{4}$$

where K_t is assumed to be invertible (or at least has a pseudo inverse). The NGS six-thruster ROV is amenable to this framework. Additionally, let $\boldsymbol{\Delta\nu} = \boldsymbol{\nu} - \boldsymbol{\nu}_d$ and $\boldsymbol{\Delta\eta} = \boldsymbol{\eta} - \boldsymbol{\eta}_d$ convert the state-space equations into error coordinates relative to known reference attitude and velocity setpoints $\boldsymbol{\nu}_d$ and $\boldsymbol{\eta}_d$ obtainable from user inputs. Assume $\dot{\boldsymbol{\nu}}_d$ is readily known and continuous.

The proportional gain matrix $K_P(\boldsymbol{\eta})$ is a 6×3 matrix varying with vehicle orientation relative to the Earth-fixed

frame. The derivative gain matrix K_D is a constant positive-definite symmetric matrix. The control law (4) yields the closed-loop dynamics [6]

$$\frac{d}{dt}(\boldsymbol{\Delta\nu}) = -K_P(\boldsymbol{\eta})\boldsymbol{\Delta\eta} - K_D\boldsymbol{\Delta\nu} \tag{5}$$

$$\frac{d}{dt}(\boldsymbol{\Delta\eta}) = J(\boldsymbol{\eta})\boldsymbol{\Delta\nu}, \tag{6}$$

which asymptotically stabilize the origin $\boldsymbol{\Delta\nu} = 0$ and $\boldsymbol{\Delta\eta} = 0$ [6].

III. THRUSTER DYNAMICS AND CONTROL

A. Dynamic Thruster Model with an Input Dead Zone

The control law in (4) defines a desired set of actuator thrusts that stabilize the closed-loop setpoint-tracking dynamics of the ROV. Thrust can be related to the propeller angular velocity of an ROV thruster by a dead zone function [8]

$$T(n) = \begin{cases} k_{T1}(n|n| - \delta_{T1}), & n|n| \le \delta_{T1} \\ 0, & \delta_{T1} < n|n| < \delta_{T2} \\ k_{T2}(n|n| - \delta_{T2}), & n|n| \ge \delta_{T2}, \end{cases} \tag{7}$$

where n represents propeller angular velocity, the constants k_{T1}, k_{T2}, and δ_{T2} are positive, and δ_{T1} is negative. In order to determine the desired propeller angular velocity n_d for a desired thrust T_d, inverting the dead zone function (7) yields [8]

$$n_d = \begin{cases} \mathrm{sgn}(T_d)\sqrt{|\frac{T_d}{k_{T1}} + \delta_{T1}|}, & T_d < 0 \\ 0, & T_d = 0 \\ \mathrm{sgn}(T_d)\sqrt{|\frac{T_d}{k_{T2}} + \delta_{T2}|}, & T_d > 0. \end{cases} \tag{8}$$

The desired propeller angular velocity n_d is fed back into a control scheme for the actuator dynamics. Bessa et al. [8] propose the following voltage-driven dynamic model for an ROV thruster:

$$\dot{n} = -k_1 n - k_2 n|n| + k_v u, \tag{9}$$

where u is the input motor voltage and the constants k_1, k_2, and k_v are positive. Equation (9) is a single-state thruster model that is valid at low propeller speeds [8].

We consider an alternate version of (9) that, instead of being driven by a direct motor voltage, is controlled by an analog voltage throttle signal with a dead zone around zero volts. The new model is

$$\dot{n} = -k_1 n - k_2 Q(n) + \gamma(u), \tag{10}$$

where $Q(n)$ is the reaction torque on the propeller, and the function $\gamma(u)$ relates throttle signal u to motor torque by a dead zone function

$$\gamma(u) = \begin{cases} k_{v1}(u - \delta_{v1}), & u \le \delta_{v1} \\ 0, & \delta_{v1} < u < \delta_{v2} \\ k_{v2}(u - \delta_{v2}), & u \ge \delta_{v2}. \end{cases} \tag{11}$$

The effects of the nonlinear function (11) on (10) are presented in Fig. 3 by plotting steady-state propeller speed data as a function of the constant throttle voltages that drive the system to those operating points. A fit based on (10) is also plotted to validate the accuracy of the model. Note that (11) can be inverted as

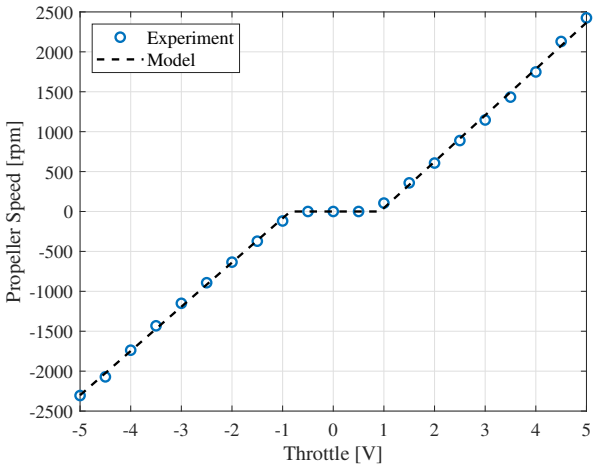

Fig. 3. Steady-state propeller angular velocity data from [20] resulting from constant throttle inputs show the nonlinear dead zone behavior of the model (10).

$$\gamma^{-1}(\alpha) = \begin{cases} k_{v1}^{-1}\alpha + \delta_{v1}, & \alpha < 0 \\ 0, & \alpha = 0 \\ k_{v2}^{-1}\alpha + \delta_{v2}, & \alpha > 0, \end{cases} \tag{12}$$

for any generic commanded motor torque α.

In (10), Q represents the collected inertial and hydrodynamic reaction torque enacted on the thrusters, which is often a quadratic function of n, and may be defined with a dead zone similar to (7), i.e.,

$$Q(n) = \begin{cases} k_{Q1}(n|n| - \delta_{Q1}), & n|n| \le \delta_{Q1} \\ 0, & \delta_{Q1} < n|n| < \delta_{Q2} \\ k_{Q2}(n|n| - \delta_{Q2}), & n|n| \ge \delta_{Q2}, \end{cases} \tag{13}$$

with positive constants k_{Q1}, k_{Q2}, and δ_{Q2}, and negative constant δ_{Q1}. Steady-state thrust and torque data of a thruster [20] were used to identify the parameters in the models (7) and (13). The models were fit to these data as shown in Fig. 4.

B. Feedback-Linearizing Control Design

To drive the dynamics (10) to a known setpoint n_d we use the inverse dead zone function (12) and feedback linearization to derive a control law that compensates for nonlinearities in the thruster dynamics. We show below that this framework exponentially stabilizes $n = n_d$.

Theorem 1: Assuming u can change instantaneously, the dynamics (10) exponentially stabilize the setpoint $\Delta n = n - n_d = 0$ using the control law

$$u = \gamma^{-1}(\alpha), \tag{14}$$

where $\gamma^{-1}(\alpha)$ is defined in (12) and

$$\alpha = \dot{n}_d + k_1 n + k_2 Q(n) - k_u \Delta n, \tag{15}$$

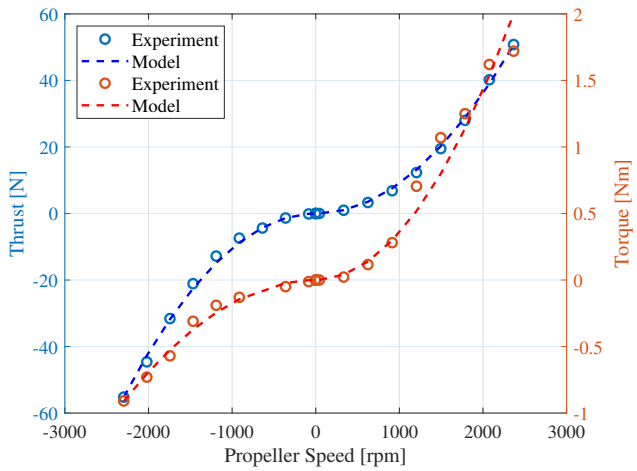

Fig. 4. Steady-state thruster model compared to experimental data from [20] for thrust and torque.

for $k_u > 0$.

Proof: Consider the scenario where the system is operating under the first condition in (12), i.e., $\alpha < 0$. Therefore, (10) becomes

$$\begin{aligned}\dot{n} &= -k_1 n - k_2 Q(n) + \dot{n}_d + k_1 n + k_2 Q(n) - k_u \Delta n \\ &= \dot{n}_d - k_u \Delta n,\end{aligned} \tag{16}$$

which implies

$$\frac{d}{dt}(\Delta n) = -k_u \Delta n. \tag{17}$$

Equation (17) is a scalar Hurwitz linear system in error coordinates relative to the setpoint n_d.

The same steps yield identical results for the third condition of (12), so operating on either end of the dead zone yields the system (17). In the case that $\alpha = 0$, substituting (15) into (10) also yields (17), which completes the proof. ■

If perfect knowledge of $\dot{n}_d$ is not available in practice, a piecewise constant estimate may be used in its place. We observe the following result.

Corollary 1.1: Let $\delta > 0$. Using the estimate $\hat{\dot{n}}_d = \dot{n}_d + \epsilon$, where the estimation error ϵ satisfies $|\epsilon| < \delta$, the solution to the closed-loop dynamics (17) using the control law (14) is bounded by $|\Delta n| \leq \delta / k_u$.

Proof: With the estimate $\hat{\dot{n}}_d = \dot{n}_d + \epsilon$, (17) becomes

$$\frac{d}{dt}(\Delta n) = -k_u \Delta n + \epsilon. \tag{18}$$

The time-derivative of the quadratic Lyapunov function $V = (\Delta n)^2/2$ along solutions of (18) satisfies

$$\dot{V} \leq -k_u (\Delta n)^2 + |\Delta n| \delta, \tag{19}$$

which implies the closed-loop dynamics (17) converge to $|\Delta n| \leq \delta / k_u$. ■

In practice, physical thrusters have a maximum ramp speed, i.e., u cannot change instantaneously, which limits the convergence rate to the desired setpoint. We model this limitation as a maximum allowable throttle change rate, i.e., $\dot{u}_{max}$. Since u cannot change instantaneously, it may pass through the dead zone. The maximum amount of time the motor spends in the dead zone while transitioning to a thruster operating point outside the dead zone is

$$t_{max} = \frac{\delta_{v2} - \delta_{v1}}{\dot{u}_{max}} > 0. \tag{20}$$

During this time, the dynamics (10) will be unforced, requiring additional analysis of the system in this scenario.

Theorem 2: Consider the dynamics (10). When u is within the throttle dead zone, the zero-input dynamics

$$\dot{n} = -k_1 n - k_2 Q(n) \tag{21}$$

exponentially stabilize the origin $n = 0$.

Proof: We analyze the stability properties of the unforced system (21) with the quadratic Lyapunov function

$$V = \frac{1}{2} n^2, \tag{22}$$

which varies according to

$$\dot{V} = -k_1 n^2 - k_2 Q(n) n. \tag{23}$$

Equation (23) can take one of three forms depending on the value of n. Because the constants k_1 and k_2 are positive, $\dot{V}$ is negative definite if $Q(n)n$ is positive semi-definite for all n. According to (13), $Q(n)$ either has the same sign as n or is zero for $\delta_{Q1} < n|n| < \delta_{Q2}$, because k_{Q1}, k_{Q2}, and δ_{Q2} are all positive and δ_{Q1} is negative. We therefore conclude $Q(n)n$ is positive semi-definite, and $\dot{V}$ is negative definite for all n. Note that $k_a n^2 \leq V \leq k_b n^2$ and $\dot{V} \leq -k_1 n^2$ for $k_b > 0.5 > k_a > 0$, which implies that the unforced system (21) exponentially stabilizes the origin. ■

The thruster motor operates in the dead zone in one of only three scenarios: during startup, wind-down, or a transition between forward and reverse thrust. In all of these scenarios, convergence to zero propeller speed is either advantageous or inconsequential (as in the case of motor startup). Typically t_{max} in (20) is on the order of tens of milliseconds, whereas the wind-down time for an ROV thruster was experimentally observed to be as much as half a second [20]. As a result, crossing the throttle dead zone is not predicted to destabilize the physical system during regular operation. Fig. 5 depicts a simulation of the dead-zone-compensating controller (14) successfully driving the actuator dynamics from multiple operating points of n to a positive setpoint value of n_d, taking into account the limitation $|\dot{u}| \leq \dot{u}_{max}$.

IV. FULL MODEL AND SIMULATION RESULTS

With analysis of the capabilities of the thruster control design complete, we further verify its performance with full system simulations. The systems in (1), (2), and (10) represent the full system dynamics of the ROV, including rigid-body dynamics and uncoupled actuator dynamics for each thruster, i.e.,

$$\dot{\boldsymbol{x}} = \boldsymbol{f}(\boldsymbol{x}) + \boldsymbol{g}(\boldsymbol{u}), \tag{24}$$

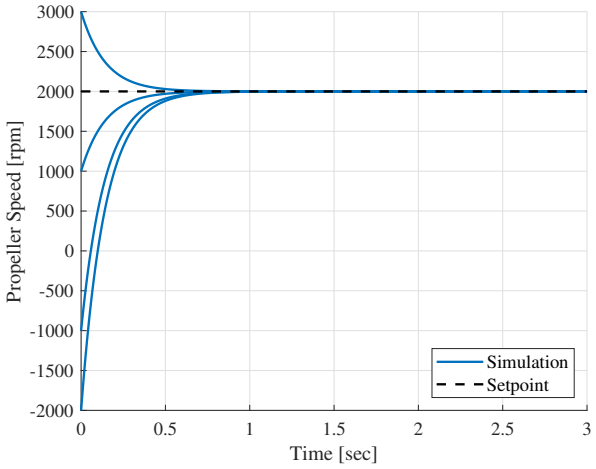

Fig. 5. Simulations of the dead-zone-compensating controller driving a thruster from multiple operating points to a positive setpoint with consideration for $\dot{u}_{max}$.

where $\boldsymbol{x} = [\boldsymbol{\eta}^T \ \boldsymbol{\nu}^T \ \boldsymbol{n}^T]^T$ and $\boldsymbol{n}$ is the vector of the (six) thruster states of the ROV. The vector fields $\boldsymbol{f}(\boldsymbol{x})$ and $\boldsymbol{g}(\boldsymbol{u})$ are

$$\boldsymbol{f}(\boldsymbol{x}) = \begin{bmatrix} J(\boldsymbol{\eta})\boldsymbol{\nu} \\ M^{-1}[K_t \boldsymbol{T}(\boldsymbol{n}) - C(\boldsymbol{\nu})\boldsymbol{\nu} - D(\boldsymbol{\nu})\boldsymbol{\nu} - \boldsymbol{g}(\boldsymbol{\eta})] \\ -K_n \boldsymbol{n} - K_Q \boldsymbol{Q}(\boldsymbol{n}) \end{bmatrix}, \tag{25}$$

and $\boldsymbol{g}(\boldsymbol{u}) = [0 \cdots 0 \ \boldsymbol{\gamma}(\boldsymbol{u})]^T$, where K_n and K_Q are diagonal matrices containing the parameters of the dynamics from (10) for each individual thruster. The closed-loop dynamics take the form

$$\frac{d}{dt}\begin{bmatrix} \boldsymbol{\Delta\eta} \\ \boldsymbol{\Delta\nu} \\ \boldsymbol{\Delta n} \end{bmatrix} = \begin{bmatrix} J(\boldsymbol{\eta})\boldsymbol{\Delta\nu} \\ -K_P(\boldsymbol{\eta})\boldsymbol{\Delta\eta} - K_D\boldsymbol{\Delta\nu} \\ -K_u \boldsymbol{\Delta n} \end{bmatrix} \tag{26}$$

where K_u is the diagonal matrix of feedback gains.

Theorem 3: The full closed-loop dynamics for the ROV (26) asymptotically stabilize the origin $\boldsymbol{\Delta x} = \boldsymbol{x} - \boldsymbol{x}_d = 0$.

Proof: The system (26) combines the dynamics in (1) and (2), which asymptotically stabilize the origin $\boldsymbol{\Delta\nu} = 0$ and $\boldsymbol{\Delta\eta} = 0$, with the dynamics of the thrusters (10) which are fully uncoupled and each exponentially stabilize the origin $\boldsymbol{\Delta n} = 0$. Therefore, because each sub-system is asymptotically stable, the full closed-loop system asymptotically stabilizes the origin $\boldsymbol{\Delta x} = 0$. ■

Simulations of the system (24) verify the setpoint-tracking performance of the dead-zone-compensating controller (14) when implemented in a full-vehicle scenario. Tracking performance of the control scheme compares favorably to a lookup table that is based solely on data presented in Fig. 3. The lookup table determines the control input that drives a thruster to the desired steady-state propeller angular velocity. This method does not account for actuator dynamics, and assumes rapid convergence to steady-state propeller speed.

Fig. 6 indicates superior performance of the dead-zone-compensating controller over the lookup-table method. The tracking task involves varying setpoints in forward velocity u, pitch rate q, and pitch θ. Parameter values used in simulation of the thruster dynamics are reported in Table I. Physical parameters for the thrusters were determined via system identification methods using a six-axis Gough-Stewart platform load cell [20].

To further compare performance of the control methods, the root-mean-square tracking error (RMSE) was calculated for each degree of freedom over the course of the simulation time period and normalized by the average value of each respective degree of freedom. Normalized RMSE results are presented in Fig. 7. The dead-zone-compensating controller displays comparable tracking performance in linear velocities when compared to the lookup-table method, but significant improvement comes in tracking attitude and angular velocity setpoints, with tracking errors being reduced by as much as 50%. Divergence from the reference setpoint displayed in the performance of the lookup-table controller is attributed to the trade-off of tracking forward velocity with the other states, as multiple setpoints were processed simultaneously.

V. CONCLUSION

This paper presents a modeling and control framework for using feedback-linearizing control methods on throttle-driven ROV thrusters that have input dead zones. Compensating the nonlinearities in the actuator dynamics achieves better setpoint tracking performance in simulation when compared to lookup-table control methods that do not account for thruster dynamics. Overall the use of feedback linearization to stabilize both the rigid-body vehicle dynamics and the thruster behavior is effective as long as sufficient knowledge of model parameters is available. Ongoing work seeks to extend this framework to a two-state model of thruster dynamics with the inclusion of axial flow as an unmeasured state. Current and future control schemes will support upcoming field trials with the NGS ROV.

TABLE I
THRUSTER MODEL PARAMETER VALUES

Parameter	Value	Units
k_{T1}	1.047×10^{-5}	N·rpm^{-2}
k_{T2}	9.045×10^{-6}	N·rpm^{-2}
δ_{T1}	-2.919	rpm^2
δ_{T2}	0.1994	rpm^2
k_{Q1}	1.729×10^{-7}	N·m·rpm^{-2}
k_{Q2}	3.570×10^{-7}	N·m·rpm^{-2}
δ_{Q1}	-1.962	rpm^2
δ_{Q2}	1.748	rpm^2
k_{v1}	7578	rpm·(V·s)$^{-1}$
k_{v2}	6770	rpm·(V·s)$^{-1}$
δ_{v1}	-0.8475	V
δ_{v2}	0.9254	V
k_1	11.30	s^{-1}
k_2	646.1	rpm·(N·m·s)$^{-1}$
$\dot{u}_{max}$	100	V·s^{-1}

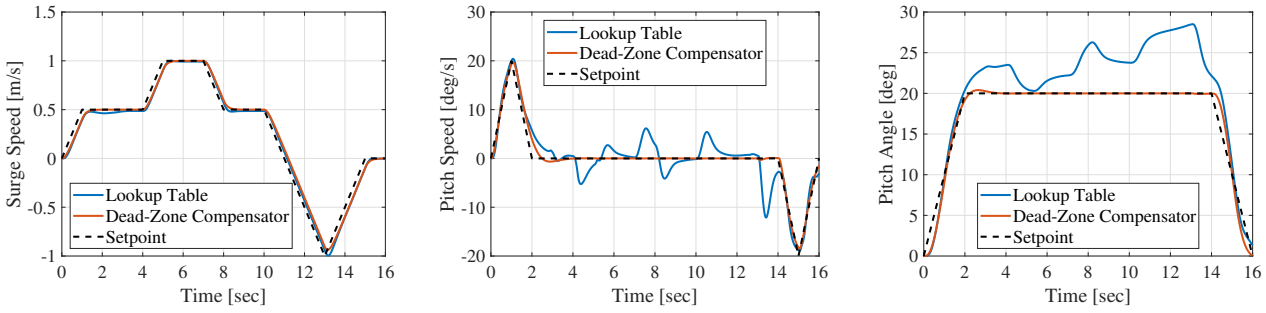

(a) (b) (c)

Fig. 6. Setpoint tracking performance comparison between the proposed dead-zone-compensating controller and thrust-table-based control for (a) linear forward velocity, (b) angular pitch velocity, and (c) pitch angle.

ACKNOWLEDGMENT

The authors would like to thank Arthur Clarke, Alan Turchik, and Cody Goldhahn of the National Geographic Society for their assistance with thruster testing and data collection.

REFERENCES

[1] M. Ludvigsen, F. Søreide, K. Aasly, S. Ellefmo, M. Zylstra, and M. Pardey, "ROV based drilling for deep sea mining exploration," in *OCEANS Aberdeen*, June 2017, pp. 1–6.

[2] R. Nian, B. He, J. Yu, Z. Bao, and Y. Wang, "ROV-based underwater vision system for intelligent fish ethology research," *International Journal of Advanced Robotic Systems*, vol. 10, no. 9, p. 326, 2013.

[3] S. Negahdaripour and P. Firoozfam, "An ROV stereovision system for ship-hull inspection," *IEEE Journal of Oceanic Engineering*, vol. 31, no. 3, pp. 551–564, July 2006.

[4] S. M. Nornes, M. Ludvigsen, Ø. Ødegard, and A. J. Sørensen, "Underwater photogrammetric mapping of an intact standing steel wreck with ROV," *IFAC-PapersOnLine*, vol. 48, no. 2, pp. 206 – 211, 2015.

[5] R. D. Christ and R. L. Wernli, *The ROV Manual: A User Guide for Remotely Operated Vehicles*, 2nd ed. Waltham, MA, USA: Elsevier, 2014.

[6] S. C. Martin and L. L. Whitcomb, "Preliminary experiments in fully actuated model based control with six degree-of-freedom coupled dynamical plant models for underwater vehicles," in *IEEE International Conference on Robotics and Automation*, May 2013, pp. 4621–4628.

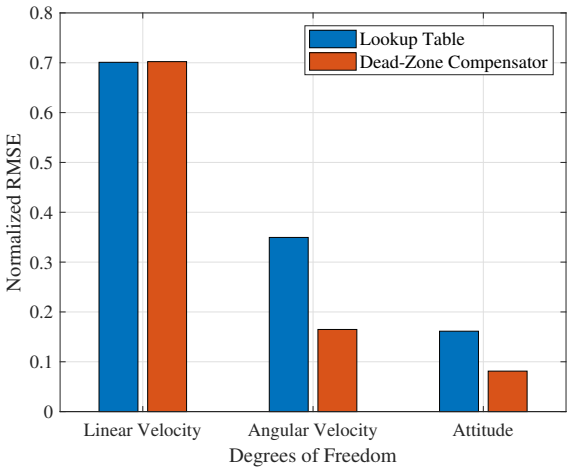

Fig. 7. Tracking errors for each degree of freedom involved in setpoint tracking.

[7] ——, "Nonlinear model-based tracking control of underwater vehicles with three degree-of-freedom fully coupled dynamical plant models: Theory and experimental evaluation," *IEEE Transactions on Control Systems Technology*, vol. 26, no. 2, pp. 404–414, March 2018.

[8] W. M. Bessa, M. S. Dutra, and E. Kreuzer, "Dynamic positioning of underwater robotic vehicles with thruster dynamics compensation," *International Journal of Advanced Robotic Systems*, vol. 10, no. 9, p. 325, 2013.

[9] L. G. Garca-Valdovinos, T. Salgado-Jimnez, M. Bandala-Snchez, L. Nava-Balanzar, R. Hernndez-Alvarado, and J. A. Cruz-Ledesma, "Modelling, design and robust control of a remotely operated underwater vehicle," *International Journal of Advanced Robotic Systems*, vol. 11, no. 1, p. 1, 2014.

[10] P.-M. Lee, B.-H. Jeon, S.-W. Hong, Y.-K. Lim, C.-M. Lee, J.-W. Park, and C.-M. Lee, "System design of an ROV with manipulators and adaptive control of it," in *Proceedings of the International Symposium on Underwater Technology*, May 2000, pp. 431–436.

[11] H. D. Nguyen, S. Malalagama, and D. Ranmuthugala, "Design, modelling and simulation of a remotely operated vehicle–Part 1," *Journal of Computer Science and Cybernetics*, vol. 29, no. 4, pp. 299–312, 2013.

[12] L. L. Whitcomb and D. R. Yoerger, "Development, comparison, and preliminary experimental validation of nonlinear dynamic thruster models," *IEEE Journal of Oceanic Engineering*, vol. 24, no. 4, pp. 481–494, Oct 1999.

[13] A. J. Healey, S. M. Rock, S. Cody, D. Miles, and J. P. Brown, "Toward an improved understanding of thruster dynamics for underwater vehicles," in *Proceedings of IEEE Symposium on Autonomous Underwater Vehicle Technology*, July 1994, pp. 340–352.

[14] M. Blanke, K.-P. Lindegaard, and T. I. Fossen, "Dynamic model for thrust generation of marine propellers," *IFAC Proceedings Volumes*, vol. 33, no. 21, pp. 353 – 358, 2000.

[15] T. I. Fossen and M. Blanke, "Nonlinear output feedback control of underwater vehicle propellers using feedback form estimated axial flow velocity," *IEEE Journal of Oceanic Engineering*, vol. 25, no. 2, pp. 241–255, April 2000.

[16] R. Bachmayer, L. L. Whitcomb, and M. A. Grosenbaugh, "An accurate four-quadrant nonlinear dynamical model for marine thrusters: theory and experimental validation," *IEEE Journal of Oceanic Engineering*, vol. 25, no. 1, pp. 146–159, Jan 2000.

[17] J. Kim, "Thruster modeling and controller design for unmanned underwater vehicles (UUVs)," in *Underwater Vehicles*, A. V. Inzartsev, Ed. Rijeka: IntechOpen, 2009, ch. 13.

[18] X. Wu, X. Wu, and X. Luo, "Adaptive control of nonlinearly parameterized system with unknown dead-zone input," in *8th World Congress on Intelligent Control and Automation*, July 2010, pp. 3811–3815.

[19] N. F. Jasim and I. F. Jasim, "Robust control design for spacecraft attitude systems with unknown dead zone," in *IEEE International Conference on Control System, Computing and Engineering*, Nov 2011, pp. 375–380.

[20] J. Boehm, E. Berkenpas, B. Henning, M. Rodriguez, C. Shepard, and A. Turchik, "Characterization, modeling, and simulation of an ROV thruster using a six degree-of-freedom load cell," in *OCEANS 2018 MTS/IEEE Charleston*, Oct 2018, pp. 1–7.

[21] T. Fossen, *Guidance and control of ocean vehicles*. Wiley, 1994.